Arabian Journal for Science and Engineering (2025) 50:17369–17379
https://doi.org/10.1007/s13369-024-09934-2

RESEARCH ARTICLE-ELECTRICAL ENGINEERING

Neural Network-Based Finite-Time Control for Stochastic Nonlinear Systems with Input Dead-Zone and Saturation

Mohamed Kharrat[1] · Moez Krichen[2] · Hadil Alhazmi[3] · Paolo Mercorelli[4]

Received: 15 July 2024 / Accepted: 23 December 2024 / Published online: 11 January 2025

Abstract
The problem of adaptive control for stochastic systems impacted by saturation and dead zone is discussed in this study. Neural networks are incorporated into the design to effectively control the unknown nonlinear functions present in these systems. The non-smooth input saturation and dead-zone nonlinearities are approximated using the non-affine smooth function. Next, the mean-value theorem is applied to derive the affine form. The study develops an adaptive finite-time controller using the backstepping approach, ensuring semi-globally practical finite-time stability for all closed-loop system signals while driving the tracking error to converge within a finite time to a small region around the origin. To illustrate the efficacy of the suggested control strategy, two simulation examples are given.

Keywords Nonlinear systems · Stochastic systems · Dead-zone · Saturation · Finite-time stability

1 Introduction

In recent decades, with the prevalence of nonlinear systems in real-world applications, there has been a significant shift in attention among experts and scholars toward addressing the control challenges posed by these systems [1–3]. Traditional linear control methods are often insufficient for direct application, prompting the exploration of alternative approaches. Among these, adaptive backstepping control has emerged as an effective and influential control scheme in both theoretical and engineering domains. Its key advantage lies in the ability to dynamically adjust parameters through online learning. This attribute has contributed to its widespread adoption in the design of controllers for various practical systems, owing to its exceptional performance. Stochastic disturbances, frequently encountered in various practical nonlinear systems, pose a challenge in synthesizing controls, adding complexity to the process [4, 5]. This necessitates the consideration of these uncertainties in control strategies, further emphasizing the relevance and applicability of adaptive backstepping control in addressing the challenges posed by nonlinear systems subjected to stochastic disturbances [6]. The presence of stochastic disturbances can potentially lead to system instability and suboptimal performance. Consequently, these disturbances must be incorporated into the modeling and analysis processes. Addressing the impact of stochastic disturbances on system stability and control performance has become a significant and increasingly explored area of research [7, 8]. To tackle this issue, researchers have delved into control design methodologies for stochastic nonlinear systems [9]. One notable approach involves integrating adaptive control techniques with linear matrix inequality methods, leading to the development of a disturbance observer-based approach tailored for stochastic systems [10]. In a different context, a sliding mode controller has been devised specifically for singular stochastic Markov jump systems [11]. Additionally, for stochastic nonlinear high-order systems, a state-feedback control law was designed to ensure effective control and stability [12].

Nevertheless, the previously mentioned control strategies may prove ineffective when applied to stochastic systems

✉ Paolo Mercorelli
paolo.mercorelli@leuphana.de

[1] Mathematics Department, College of Science, Jouf University, Sakaka, Saudi Arabia

[2] Al-Baha University, Al-Baha 65528, Saudi Arabia ReDCAD Laboratory, University of Sfax, Sfax 3038, Tunisia

[3] Department of Mathematical Sciences, College of Science, Princess Nourah Bint Abdulrahman University, 84428, 11671 Riyadh, Saudi Arabia

[4] Institute for Production Technology and Systems, Leuphana University of Lueneburg, Universitaetsallee 1, 21335 Lueneburg, Germany

featuring unknown nonlinear functions. These methods often rely on the precise knowledge of nonlinear dynamics models or assume that unknown parameters exhibit linearity concerning known nonlinear functions [13, 14]. In light of these challenges, numerous scholars have dedicated substantial efforts to developing approximation-based adaptive control using fuzzy logic or neural networks for different classes of nonlinear systems. Utilizing the impressive function estimation powerful capacity of neural networks (NNs) or fuzzy logical systems (FLSs), these techniques have found widespread application in the control of nonlinear systems [15, 16]. For instance, researchers have addressed adaptive control challenges in stochastic nonlinear systems by incorporating prescribed performance criteria [17]. Furthermore, an observer-based adaptive control technique has been specifically designed to handle systems constrained by both input and state limitations [18]. Furthermore, research efforts have been focused on crafting adaptive dynamic surface control strategies specifically designed for nonstrict-feedback constrained nonlinear stochastic systems [19]. In [20], an adaptive control mechanism was developed via observer for switched systems using the average dwell time approach. An adaptive fuzzy control approach is introduced for handling nonlinear systems with a multi-input multi-output configuration, focusing on the challenge of partial constraints on tracking errors [21].

Input saturation has emerged as a noteworthy source of instability and performance degradation in practical systems, garnering considerable attention. The extensive research in this area underscores that control systems facing input saturation can result in inaccuracies or, in more severe cases, instability. Therefore, it becomes imperative to consider and address input saturation when designing controllers for practical applications in industrial process control [22]. Over time, substantial progress has been made in addressing this challenge, resulting in noteworthy achievements in the design of controllers for systems subjected to input saturation [23, 24]. For example, within the domain of switched stochastic systems in pure-feedback form encountering input saturation, there is documentation of an adaptive control scheme utilizing neural networks and observers [25]. A notable breakthrough includes the development of an adaptive control method for nonlinear stochastic systems, which addresses both time-varying state constraints and input saturation. This approach integrates neural networks for efficient approximation, as reported in [26]. Furthermore, in the realm of fractional-order nonlinear systems with nonstrict-feedback nature, an adaptive neural network control approach was introduced to manage full-state constraints and input saturation, as detailed in [27]. These innovative control strategies underscore the importance of addressing input saturation in practical systems, showcasing the versatility of neural networks in overcoming the challenges associated with this nonlinearity.

On the other side, the influence of dead-zone input, a widespread nonlinearity in control systems, has been encountered in practical applications such as electric servomotors, electronic circuits, and hydraulic and pneumatic valves [28]. This nonlinearity has the potential to degrade system performance and even lead to instability. Fortunately, a range of control methods has been devised to alleviate the detrimental effects of dead-zone input, providing solutions for systems affected by this phenomenon [29, 30]. For example, within the domain of nonlinear systems affected by control directions and input dead-zones, researchers have presented an adaptive control approach, leveraging the approximation capabilities of neural networks to address the challenges posed by dead-zone input [31]. For switched nonlinear systems, neural networks have been used to approximate unknown functions effectively [32]. In stochastic systems, adaptive neural control strategies have been designed to handle dead-zone nonlinearities [33]. One example deals with stochastic systems facing unmodeled dynamics and time-varying delays, using an adaptive neural control approach [34]. An alternative approach addresses nonstrict-feedback stochastic systems with dead zones by employing output feedback in adaptive control [35]. For strict-feedback stochastic systems encountering dead zones, performance is enhanced by neural control techniques paired with command filters [36]. In pure-feedback nonlinear systems affected by dead zones, adaptive dynamic surface control has been implemented [37]. Furthermore, observer-based adaptive fuzzy control has been applied to large-scale switched systems with dead zones [38]. Lastly, a control strategy for nonstrict-feedback systems with multiple actuator constraints, including input dead zones and saturation, integrates neural networks and command filters for improved performance [39].

It is important to note that the earlier results primarily emphasize asymptotic stability, which assumes that the system will stabilize as time approaches infinity. However, in real-world applications, achieving control goals within a finite and timely manner is often more critical. Finite-time convergence becomes a key consideration, prompting researchers and control engineers to develop advanced control methods tailored to time-limited scenarios [40]. The exploration of finite-time stabilization or tracking control for nonlinear stochastic systems has garnered significant attention in recent decades [41]. For instance, to handle stochastic nonlinear systems with input saturation and full-state constraints, an adaptive finite-time control technique has been presented [42]. Employing fuzzy approximation, another study has tackled stochastic nonlinear systems experiencing actuator faults, introducing an adaptive control approach designed for finite-time convergence [43]. Additionally, an

adaptive finite-time control method has been reported for stochastic nonlinear systems with unmodeled dynamics, utilizing an event-trigger mechanism [44].

Notably, little research has been done on the adaptive finite-time control tracking problem for stochastic nonlinear systems with dead-zone input and saturation. This research gap is what inspired us to do our current investigation. It draws attention to the necessity of deepening and broadening our understanding of adaptive finite-time control strategies created especially for stochastic nonlinear systems that must overcome input constraints related to saturation and dead zones. To this end, the work is centered on the adaptive finite-time control problem for stochastic nonlinear systems with dead zone and saturation. The main contribution is summarized as follows:

1. To reduce the negative consequences of saturation and dead-zone in stochastic nonlinear systems, a finite-time adaptive controller is constructed. Additionally, the systems formulated in nonstrict-feedback forms are considered more universal compared to strict-feedback and pure-feedback structures due to their irregular system architecture. From this perspective, the considered system is deemed more suitable for realistic applications.
2. By simultaneously taking into account input saturation and dead zone in control techniques, this article differs from earlier research [24, 30, 32]. Moreover, a non-affine smooth function mimics the non-smooth characteristics of this input saturation and dead-zone nonlinearities. The mean-value theorem transforms these non-smooth features into an affine form. By using this approach, the suggested approaches become more flexible and efficient, providing a special way to deal with the problems caused by non-smooth nonlinearities in real-world control systems.

The remainder of the paper is structured as follows: Section 2 covers the system description and introduces preliminary concepts. Section 3 outlines the design of the finite-time adaptive controller. Section 4 presents two simulation examples, and Sect. 5 concludes the paper.

2 System Description and Preliminaries

Consider the stochastic nonlinear systems with saturation and dead zone

$$\begin{cases} dx_i = (x_{i+1} + f_i(x))dt + \psi_i^T(x)dw, \quad 1 \le i \le n-1, \\ dx_n = (\lambda + f_n(x))dt + \psi_n^T(x)dw, \\ y = x_1, \end{cases} \tag{1}$$

where $x = [x_1, x_2, \ldots, x_n]^T \in \mathbb{R}^n$ is the state vector, $\lambda \in \mathbb{R}$ represents the system input, and $y \in \mathbb{R}$ is the output. The functions f_i and ψ_i $(i = 1, 2, \ldots, n)$ denote unknown nonlinear terms, and w represents an r-dimensional standard Brownian motion. The input λ is affected by dead-zone and saturation nonlinearities, which are described as follows [39]:

$$\lambda = \begin{cases} \lambda_H, & \text{if } v > \lambda_H \\ l + (v - \lambda^+), & \text{if } \lambda^+ < v < \lambda_H \\ 0, & \text{if } -\lambda^- < v < \lambda^+ \\ l - (v + \lambda^-), & \text{if } -\lambda_L < v < -\lambda^- \\ -\lambda_L, & \text{if } v < -\lambda_L \end{cases} \tag{2}$$

where v represents the control input, $l^+ > 0$, $\lambda^+ > 0$, $l^- < 0$, $\lambda^- < 0$ denote constants, and $\lambda_H > 0$, $\lambda_L > 0$ signify unknown saturation values.

Examine the stochastic system defined by

$$dx = f(x, \lambda)\, dt + \psi^T(x, \lambda)\, dw, \tag{3}$$

where w is a r-dimensional Brownian motion defined on the probability space $(\Omega, \mathcal{F}, \{\mathcal{F}_t\}_{t\ge 0}, \mathbb{P})$. Let $x \in \mathbb{R}^n$ represent the system's state. In this instance, the sample space is denoted by Ω, the σ-field is denoted by $\mathcal{F}_t\}_{t\ge 0}$ by the filtering, and the probability measure is denoted by $\mathbb{P}$. The functions $f : \mathbb{R}^{n+m} \to \mathbb{R}^n$ and $\psi : \mathbb{R}^{n+m} \to \mathbb{R}^{n\times r}$ are assumed to be continuous and Borel measurable. The input to the system is represented by $\lambda \in \mathbb{R}^m$. These functions also meet the requirements $f(0, 0) = 0$ and $\psi(0, 0) = 0$.

Definition 1 [40] For any $V(x) \in C^2$, define a differential operator as

$$LV = \frac{\partial V}{\partial t} + \frac{\partial V}{\partial x} f + \frac{1}{2}\mathrm{Tr}\left\{ g^T \frac{\partial^2 V}{\partial x^2} g \right\}, \tag{4}$$

with Tr being the trace of the matrix.

Definition 2 [43] The system (3) is regarded as practically finite-time stable in the mean-square sense for any initial condition $z(t_0) = z_0$ if there exists a parameter $\varepsilon > 0$ and a finite settling time $T(\varepsilon, z_0) < \infty$ such that $E(|z(t)|^2) < \varepsilon$ for all $t > t_0 + T$.

Lemma 1 [43] *For real numbers ζ_k with $0 < \sigma \le 1$, one has*

$$\left(\sum_{k=1}^{n} |\zeta_k|^\sigma \right)^{\frac{1}{\sigma}} \le n^{1-\sigma} \left(\sum_{k=1}^{n} |\zeta_k|^\sigma \right)^{\frac{1}{\sigma}}. \tag{5}$$

Lemma 2 [40] *For any real numbers α, γ, and positive constants s, v, μ, the inequality holds:*

$$|\alpha|^s |\gamma|^v \le \frac{s}{s+v}\mu|\alpha|^{s+v} + \frac{v}{s+v}\mu^{-\frac{s}{v}}|\gamma|^{s+v}. \tag{6}$$

Lemma 3 (Young's inequality) [10] *For all real numbers x and y, the subsequent inequality is valid:*

$$xy \leq \frac{q^{\kappa}}{\kappa}|x|^{\kappa} + \frac{1}{\varsigma q^{\varsigma}}|y|^{\varsigma}, \tag{7}$$

with $q > 0$, $\kappa > 1$, $\varsigma > 1$, and the relationship $(\kappa - 1)(\varsigma - 1) = 1$.

Lemma 4 [40] *For a continuous function $\psi(t)$ and $0 \leq s \leq t$, if*

$$\int_s^t \psi(\theta)\mathrm{d}\theta \leq 0, \tag{8}$$

then $\psi(t) \leq 0$ for all $t \geq 0$.

Lemma 5 [43] *For $\dot{x}(t) = f(x(t), \lambda)$, if $\exists$ a function $\rho(x(t)) \in C^2$, parameters c, σ, $d \in (0, 1)$, and functions τ_1 and τ_2 such that*

$$\begin{cases} \tau_1(|x(t)|) \leq \rho(x(t)) \leq \tau_2(|x(t)|), \\ \rho(x(t)) - \rho(x(s)) \leq -c\int_s^t \rho^{\sigma}(x(\theta))\mathrm{d}\theta \\ \quad +d(t-s), \quad \forall 0 \leq s \leq t. \end{cases} \tag{9}$$

Then $\Delta > 0$ and $\varepsilon > 0$ exist, ensuring $|x(t)| < \varepsilon$ for all $t \geq \Delta$.

Lemma 6 [10] *The RBFNN is capable of approximating the nonlinear continuous function $f(X)$ as:*

$$f(X) = W^T S(X) + \delta(X), \quad |\delta(X)| < \epsilon, \tag{10}$$

where $W = [w_1, w_2, \ldots, w_l]^T$ represents the vector of weights, and $l > 1$ denotes the count of nodes in the neural network. The vector of basis functions, $S(X) = [s_1(X), \ldots, s_l(X)]^T$, employs Gaussian functions defined by:

$$s_i(X) = \exp\left[-\frac{(X-\xi_i)^T(X-\xi_i)}{2e_i^2}\right], \quad i = 1, \ldots, l, \tag{11}$$

where ξ_i signifies the center, and $e_i > 0$ represents the width.

Lemma 7 [10] *Define $X_n = [x_1, x_2, \ldots, x_n]^T$ and $S(X_n) = [s_1(X_n), \ldots, s_l(X_n)]^T$ as the input vector and basis function vector of the RBFNN, respectively. For any positive integer m where $m \leq n$, the following relation holds:*

$$\|S(X_n)\| \leq \|S(X_m)\| \tag{12}$$

Assumption 1 [43] The target signal y_d and its first time derivative are both continuous and bounded.

Assumption 2 [39] Positive and negative dead zones have the same slope, $l^- = l^+ = l$.

Assumption 3 [39] The dead-zone parameters, λ_+, λ_-, and l, remain bounded. This implies the existence of known parameters $\lambda_{+\min}$, $\lambda_{+\max}$, $\lambda_{-\min}$, $\lambda_{-\max}$, $l_{\min}$, and $l_{\max}$ such that $\lambda_+ \in [\lambda_{+\min}, \lambda_{+\max}]$, $\lambda_- \in [\lambda_{-\min}, \lambda_{-\max}]$, and $l \in [l_{\min}, l_{\max}]$.

Through a suitable transformation, (2) can be represented as:

$$\lambda = m(v)v + \pi(v) \tag{13}$$

where $m(v)$, referred to as the dead-zone general slope, is defined as

$$m(v) = \begin{cases} \lambda_H, & \text{if } v > \lambda_H \\ l^+, & \text{if } \lambda^+ < v < \lambda_H \\ l^+, & \text{if } -\lambda^- < v < \lambda^+ \\ l^-, & \text{if } -\lambda_L < v < -\lambda^- \\ -\lambda_L, & \text{if } v < -\lambda_L \end{cases} \tag{14}$$

Furthermore, $\pi(v)$ is bounded, specifically $|\pi(v)| \leq \bar{\pi}$, where $\bar{\pi}$ serves as the upper bound.

Remark 1 The input signal v is constrained due to practical limitations. Consequently, $m(v)$ complies with the subsequent inequality

$$0 < \rho_1 \leq \min\left(\frac{\lambda_H}{v_{\max}}, l\right) \leq m(v) \leq \max\{1, l\} \tag{15}$$

with $v_{\max}$ being the maximum value of v [39].

3 Main Results

In this section, an adaptive neural network-based finite-time controller will be established for the system (1) via backstepping technique, initiated by defining the following tracking errors as

$$\zeta_1 = y - y_d, \tag{16}$$

$$\zeta_i = x_i - \alpha_{i-1}, \quad 2 \leq i \leq n, \tag{17}$$

with α_{i-1} being the virtual controller described as

$$\alpha_i = -k_i\zeta_i^{4\sigma-3} - \frac{1}{2a_i^2}\hat{\theta}_i\zeta_i^3 S_i^T(Z_i)S_i(Z_i), \tag{18}$$

with $k_i > 0$, $\sigma = \frac{4r-1}{4r+1}$ with $r \geq 2$), and $a_i > 0$ being design parameters.

The real control law is defined as:

$$v = -k_n \zeta_n^{4\sigma-3} - \frac{\hat{\theta}_n \zeta_n^3 S_n^T(Z_n) S_n(Z_n)}{2a_n^2 \rho_1}. \tag{19}$$

The formulation of the adaptive law is defined as:

$$\dot{\hat{\theta}}_i = \frac{q_i}{2a_i^2} \zeta_i^6 S_i^T(Z_i) S_i(Z_i) - \gamma_i \hat{\theta}_i, \quad \hat{\theta}_i(0) \geq 0. \tag{20}$$

with k_n, a_n, q_i, and γ_i being the positive design parameters.

Theorem 1 *Considering the stochastic nonlinear system (1) that adheres to Assumptions 1–3, it can be guaranteed that when the virtual control law (18), the real control law (19), and the adaptive law (20) are applied, the closed-loop system will attain practical finite-time stability in the mean-square sense. Additionally, the system output is assured to remain within a bounded region around the reference signal within a finite duration.*

Proof With the help of (4), one has

$$\begin{aligned} d\varsigma_1 &= (x_2 + f_1(x) - \dot{y}_d)\, dt + \psi_1^T dw, \\ d\varsigma_i &= (f_i(x) + x_{i+1} - L\alpha_{i-1})\, dt \\ &\quad + \left(\psi_i - \sum_{j=1}^{i-1} \frac{\partial \alpha_{i-1}}{\partial x_j} \psi_j\right)^T dw, \end{aligned} \tag{21}$$

$$d\varsigma_n = (f_n(x) + \lambda - L\alpha_{n-1})\, dt \tag{22}$$

$$+ \left(\psi_n - \sum_{j=1}^{n-1} \frac{\partial \alpha_{n-1}}{\partial x_j} \psi_j\right)^T dw, \tag{23}$$

where $L\alpha_{i-1} = \sum_{j=1}^{i-1} \frac{\partial \alpha_{i-1}}{\partial x_j} \left(f_j(x) + x_{j+1}\right) + \sum_{j=1}^{i-1} \frac{\partial \alpha_{i-1}}{\partial \hat{\theta}_j} \dot{\hat{\theta}}_j + \sum_{j=0}^{i-1} \frac{\partial \alpha_{i-1}}{\partial y_d^{(j)}} \frac{y_d^{(j+1)}}{2} + \frac{1}{2} \sum_{p,q=1}^{i-1} \frac{\partial^2 \alpha_{i-1}}{\partial x_p \partial x_q} \psi_p^T \psi_q.$

Consider the following stochastic Lyapunov function:

$$V(\varsigma(t)) = \sum_{i=1}^{n} \left(\frac{\varsigma_i^4}{4} + \frac{\tilde{\theta}_i^2}{2q_i}\right), \tag{24}$$

with $\tilde{\theta}_i = \theta_i - \hat{\theta}_i$ being the estimation error.

By Eqs. (4), (13), (18), (36), (37), and (38), we have

$$\begin{aligned} LV &= \varsigma_1^3(\varsigma_2 + \alpha_1 + f_1(x_1) - \dot{y}_d) + \frac{3}{2}\varsigma_1^2 \psi_1^T \psi_1 \\ &\quad + \sum_{i=1}^{n-1} \varsigma_i^3(\varsigma_{i+1} + \alpha_i + f_i(\bar{x}_i) - L\alpha_{i-1}) \\ &\quad + \sum_{i=2}^{n} \frac{3}{2}\varsigma_i^2 \left(\psi_i - \sum_{j=1}^{i-1} \frac{\partial \alpha_{i-1}}{\partial x_j} \psi_j\right)^T \\ &\quad \times \left(\psi_i - \sum_{j=1}^{i-1} \frac{\partial \alpha_{i-1}}{\partial x_j} \psi_j\right) \\ &\quad + \varsigma_n^3(f_n(\bar{x}_n) + m(v)v + \pi(v) - L\alpha_{n-1}) \\ &\quad - \sum_{i=1}^{n} \frac{1}{q_i} \tilde{\theta}_i \dot{\hat{\theta}}_i. \end{aligned} \tag{25}$$

Applying Lemma 3, we have

$$\frac{3}{2}\varsigma_1^2 \psi_1^T \psi_1 \leq \frac{3}{4} l_1^{-2} \varsigma_1^4 \|\psi_1\|^4 + \frac{3}{4} l_1^2, \tag{26}$$

$$\begin{aligned} \frac{3}{2}\varsigma_i^2 \|\psi_i - \sum_{j=1}^{i-1} \frac{\partial \alpha_{i-1}}{\partial x_j} \psi_j\|^2 &\leq \frac{3}{4} l_i^{-2} \varsigma_i^4 \|\psi_i \\ - \sum_{j=1}^{i-1} \frac{\partial \alpha_{i-1}}{\partial x_j} \psi_j\|^4 &+ \frac{3}{4} l_i^2, \end{aligned} \tag{27}$$

$$\varsigma_i^3 \varsigma_{i+1} \leq \frac{3}{4}\varsigma_i^4 + \frac{\varsigma_{i+1}^4}{4}, \tag{28}$$

$$\varsigma_n^3 \pi(v) \leq \frac{3}{4}\varsigma_n^4 + \frac{1}{4}\bar{\pi}^2, \tag{29}$$

with l_i being a positive design parameter.

By using (26)–(29) into (25), it yields

$$\begin{aligned} LV &\leq -\sum_{i=1}^{n-1} (\varsigma_i^3 \alpha_i + \varsigma_i^3 \bar{f}_i) + g(v)\varsigma_n^3 + \varsigma_n^3 \bar{f}_n - k_n \varsigma_n^{4\sigma} \\ &\quad - \sum_{i=1}^{n} \frac{3}{4}\varsigma_i^4 - \sum_{i=1}^{n} \frac{1}{q_i} \tilde{\theta}_i \dot{\hat{\theta}}_i + \sum_{i=1}^{n} \frac{3}{4} l_i^2 + \frac{1}{4}\bar{\pi}^2, \end{aligned} \tag{30}$$

where

$$\bar{f}_1 = f_1 + \frac{3}{2}\varsigma_1 + \frac{3}{4} l_1^{-2} \varsigma_1 \|\psi_1\|^4 - \dot{y}_d, \tag{31}$$

$$\begin{aligned} \bar{f}_i &= f_i - L\alpha_{i-1} + \frac{3}{4} l_i^{-2} \varsigma_i \|\psi_i - \sum_{j=1}^{i-1} \frac{\partial \alpha_{i-1}}{\partial x_j} \psi_j\|^4 \\ &\quad + \frac{7}{4}\varsigma_i, \quad (2 \leq i \leq n-1), \end{aligned} \tag{32}$$

$$\bar{f}_n = f_n - L\alpha_{n-1} + \frac{3}{4} l_n^{-2} \varsigma_n \|\psi_n - \sum_{j=1}^{n-1} \frac{\partial \alpha_{n-1}}{\partial x_j} \psi_j\|^4. \tag{33}$$

Considering $\bar{f}_i$ contains the unknown functions f_i and ψ_i, an RBFNN $W_i^T S_i(X_i)$ can be adopted to approximate $\bar{f}_i$. That is, for $\epsilon > 0$,

$$\bar{f}_i = W_i^T S_i(X_i) + \delta_i(X_i), \quad |\delta_i(X_i)| \leq \epsilon_i, \tag{34}$$

where $X_i = [x^T, \bar{\theta}_{i-1}^T, \bar{y}_d^{(i)T}]^T \in \Omega_{X_i} \subset \mathbb{R}^{3i}$ with $\bar{\theta}_{i-1} = [\hat{\theta}_1, \hat{\theta}_2, \ldots, \hat{\theta}_{i-1}]^T$, and $x = [x_1, \cdots, x_n]^T$.

Using Lemma 4 for the terms $\varsigma_i^3 \bar{f}_i$, one has

$$\varsigma_i^3 \bar{f}_i \leq \frac{1}{2a_i^2}\varsigma_i^6 \theta_i S_i^T(Z_i)S_i + \frac{1}{2}a_i^2 + \frac{3}{4}\varsigma_i^4 + \frac{1}{4}\epsilon_i^4. \tag{35}$$

where $Z_i = [\bar{x}_i^T, \bar{\theta}_{i-1}^T, \bar{y}_d^{(i)T}]^T \in \Omega_{Z_i} \subset \mathbb{R}^{3i}$ with $\bar{\theta}_{i-1} = [\hat{\theta}_1, \hat{\theta}_2, \ldots, \hat{\theta}_{i-1}]^T$, and $\bar{x}_i = [x_1, \cdots, x_i]^T$.

By using (15) and (19), we have

$$g(v)\varsigma_n^3 \leq -k_n\rho_1\varsigma_n^{4\sigma} - \frac{\varsigma_n^6 S_n^T(Z_n)S_n(Z_N)}{2a_n^2} \tag{36}$$

By using (35), (36) into (30), one has

$$LV \leq -\sum_{i=1}^{n} k_i\varsigma_i^{4\sigma} - k_n(1+\rho_1)\varsigma_n^{4\sigma} + \sum_{i=1}^{n}\frac{\gamma_i}{q_i}\tilde{\theta}_i\hat{\theta}_i + D \tag{37}$$

where $D = \sum_{j=1}^{n}\frac{1}{2a_j^2} + \frac{3}{4}l_j^2 + \frac{1}{4}\epsilon_j^4 + \frac{1}{4}\bar{\pi}^4$.

By using Lemma 3, we have

$$\frac{\gamma_i}{q_i}\tilde{\theta}_i\theta_i \leq -\frac{\gamma_i}{2q_i}\tilde{\theta}_i^2 + \frac{\gamma_i}{2q_i}\theta_i^2, \tag{38}$$

By using (38) into (37), we have

$$LV \leq -\sum_{i=1}^{n} k_i\varsigma_i^{4\sigma} - \sum_{i=1}^{n}\frac{\gamma_i}{2q_i}\tilde{\theta}_i^2 + D + \sum_{i=1}^{n}\frac{\gamma_i}{2q_i}\theta_i^2. \tag{39}$$

Let $c = \min\{k_i, \gamma_i \mid i = 1, 2, \ldots, n\}$. Then, (39) results in

$$LV \leq -c\sum_{i=1}^{n}\left(\varsigma_i^{4\sigma} + \frac{\tilde{\theta}_i^2}{2q_i}\right) + D + \sum_{i=1}^{n}\frac{\gamma_i}{2q_i}\theta_i^2. \tag{40}$$

By using Lemma 2, one has

$$\left(\sum_{i=1}^{n}\frac{\tilde{\theta}_i^2}{2q_i}\right)^{\sigma} \leq \sigma\mu + \sum_{i=1}^{n}\frac{\tilde{\theta}_i^2}{2q_i}. \tag{41}$$

By using (41) into (40), one has

$$LV \leq -4^{\sigma}c\left(\sum_{i=1}^{n}\frac{\varsigma_i^4}{4}\right)^{\sigma} - c\left(\sum_{i=1}^{n}\frac{\tilde{\theta}_i^2}{2c_i}\right)^{\sigma} + d, \tag{42}$$

with $d = c\sigma\mu + D + \sum_{i=1}^{n}\frac{\gamma_i}{2q_i}\theta_i^2$.

Applying Lemma 1, we obtain

$$LV(\varsigma(t)) \leq -cV^{\sigma}(\varsigma(t)) + d. \tag{43}$$

Utilizing (4), for $0 \leq \tau < t$, it follows that

$$\mathbb{E}V(\varsigma(t)) = \mathbb{E}V(\varsigma(\tau)) + \mathbb{E}\int_{\tau}^{t} LV(\varsigma(s))\,\mathrm{d}s = \mathbb{E}V(\varsigma(\tau)) + \int_{\tau}^{t}\mathbb{E}[LV(\varsigma(s))]\,\mathrm{d}s \tag{44}$$

Combining information from reference [40] with Jessen's inequality and utilizing (43), one has

$$\begin{aligned}\mathbb{E}[LV(\varsigma(s))] &\leq -c\mathbb{E}[V^{\sigma}(\varsigma(s))] + d \\ &\leq -c\mathbb{E}[V(\varsigma(s))]^{\sigma} + d\end{aligned} \tag{45}$$

By using (45) into (44), it yields

$$\mathbb{E}V(\varsigma(t)) \leq \mathbb{E}V(\varsigma(\tau)) + \int_{\tau}^{t}\{-c[\mathbb{E}V(\varsigma(s))]^{\sigma} + d\}\,\mathrm{d}s \tag{46}$$

Thus,

$$\begin{aligned}\mathbb{E}V(\varsigma(t)) - \mathbb{E}V(\varsigma(\tau)) \;&\leq -c\int_{\tau}^{t}[\mathbb{E}V(\varsigma(s))]^{\sigma}\,\mathrm{d}s \\ &\quad + d(t-\tau).\end{aligned} \tag{47}$$

Let $\rho(\varsigma(t)) = \mathbb{E}V(\varsigma(t))$. Utilizing Lemma 5, one can infer the existence of a settling time $\Gamma = \frac{1}{(1-\sigma)\varsigma c}(\mathbb{E}V(\varsigma(0)))^{1-\sigma}$, ensuring that $\mathbb{E}V(\varsigma(t)) \leq \varsigma$ holds for all $t \geq \Gamma$. Here, $\varsigma = 4\left(\frac{d}{(1-\varsigma)c}\right)^{\frac{1}{4\sigma}}$. The definition of $V(\varsigma(t))$ guarantees the following inequality:

$$\mathbb{E}\left(\sum_{i=1}^{n}\varsigma_i^4\right) \leq 4\mathbb{E}[V(t)] \leq 4\epsilon \quad t \geq \Gamma. \tag{48}$$

By using the characteristic of mathematical expectation, we derive

$$[\mathbb{E}(\varsigma_i^2)]^2 \leq \mathbb{E}\left(\sum_{i=1}^{n}\varsigma_i^4\right) \leq 4\epsilon, \quad t \geq \Gamma. \tag{49}$$

Furthermore,

$$\mathbb{E}(\varsigma_i^2) \leq 2\sqrt{\epsilon} \quad t \geq \Gamma. \tag{50}$$

Moreover, we have

$$\mathbb{E}(\theta_i^2) \leq 4q_{\max}\epsilon, \quad t \geq \Gamma \tag{51}$$

with $q_{\max} = \max\{q_i \mid 1 \leq i \leq n\}$.

Equations (50) and (51) together indicate that the closed system exhibits practical finite-time stability in the mean-square sense.

Remark 2 The process of selecting design parameters is generally performed through a trial-and-error approach. The overall performance of the control system is heavily influenced by the choice of controller parameters k_i, a_i, and γ_i.

Enhancing the values of k_i and γ_i, while keeping a_i as small as possible, can result in significant improvements in system behavior. However, increasing k_i may cause a rise in the magnitude of the control signals. Thus, careful adjustment and optimization of these parameters are essential to achieve the desired control performance.

4 Simulation Examples

This section demonstrates the effectiveness of the proposed control method through two simulation examples.

Example 1 Consider the following stochastic nonlinear system:

$$\begin{cases} dx_1 = \left(x_2 + (1 - \sin^2 x_1)x_2\right) dt + 0.2\cos^2 x_1\, dw, \\ dx_2 = \left(\lambda - 3.5x_2 + x_1^2 x_2^2\right) dt + 0.5\sin(2x_1x_2)\, x_2\, dw, \\ y = x_1, \end{cases} \tag{52}$$

where the state variables are denoted as x_1 and x_2, and the system input is represented by λ as defined in (2), subjected to both dead-zone and saturation effects. The reference signal is given by $y_d = \sin(0.5t) + 0.5\sin(1.5t)$. The input λ undergoes dead-zone and saturation nonlinearities defined as

$$\lambda = \begin{cases} 5, & \text{if } v > 5 \\ 0.5(v - 0.5), & \text{if } 0.5 < v < 5 \\ 0, & \text{if } -0.5 < v < 0.5 \\ 0.5(v + 0.5), & \text{if } -5 < v < 0.5 \\ -5, & \text{if } v < -5 \end{cases} \tag{53}$$

where $\lambda_H = 5$, $\lambda_L = 5$, $l = 0.5$, $\lambda^- = 0.5$, and $\lambda^+ = 0.5$.

The virtual control law, real controller, and adaptive laws are formulated as:

$$\alpha_1 = -k_1\varsigma_1^{4\sigma-3} - \frac{1}{2a_1^2}\hat{\theta}_1\varsigma_1^3 S_1^T(Z_1)S_1(Z_1), \tag{54}$$

$$v = -k_2\varsigma_2^{4\sigma-3} - \frac{\hat{\theta}_2\varsigma_2^3 S_2^T(Z_2)S_2(Z_2)}{2a_2^2\rho_1}, \tag{55}$$

$$\dot{\hat{\theta}}_i = \frac{q_i}{2a_i^2}\varsigma_i^6 S_i^T(Z_i)S_i(X_i) - \gamma_i\hat{\theta}_i, \quad i = 1, 2. \tag{56}$$

In the simulation, parameters selected using a trial-and-error approach: $q_1 = 2$, $q_2 = 4$, $a_1 = 5$, $a_2 = 1$, $\gamma_1 = 0.05$, $\gamma_2 = 0.05$, $k_1 = 10$, $k_2 = 10$, and $\sigma = \frac{99}{101}$. The initial conditions established through this method, set as $[x_1(0), x_2(0)]^T = [0.5, 0.5]^T$ and $[\hat{\theta}_1(0), \hat{\theta}_2(0)]^T = [0, 0]^T$. The simulation results are shown in Figs. 1, 2, 3, 4, and 5. Figure 1 presents the graphs for the system output y alongside the desired signal y_d. Figure 2 illustrates the tracking error ς_1. The curve for the system state x_2 is depicted in Fig. 3. Figure 4 displays the responses of the adaptive laws, while Fig. 5 illustrates both the control input v and the system input λ.

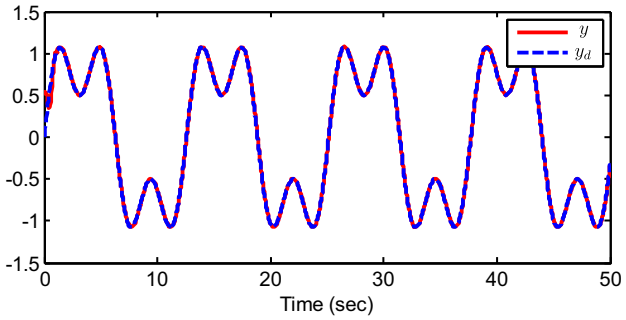

Fig. 1 Trajectories of y and y_d

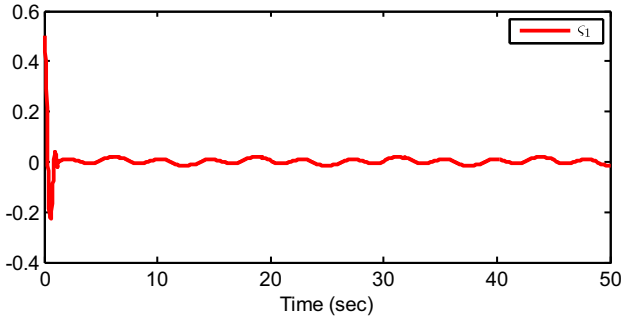

Fig. 2 The response of tracking error ς_1

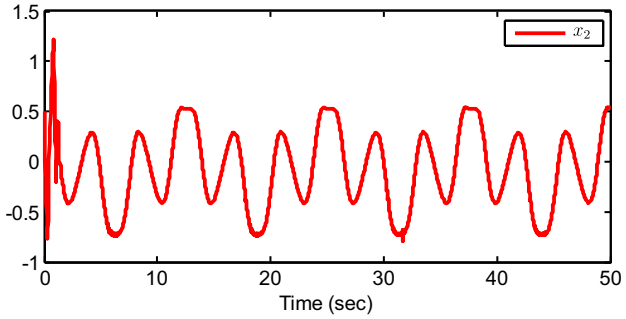

Fig. 3 The trajectories of state variable x_2

To evaluate the effectiveness of the proposed adaptive control method compared to the existing approach outlined in [18], we present the relevant results in Table 1. The performance metrics are defined as follows [45]:

$$\text{Output Index} = \sum_{k=1}^{M}[y(k) - y_d(k)]^2 \tag{57}$$

$$\text{Control Law Index} = \sum_{k=1}^{M}[v(k)]^2 \tag{58}$$

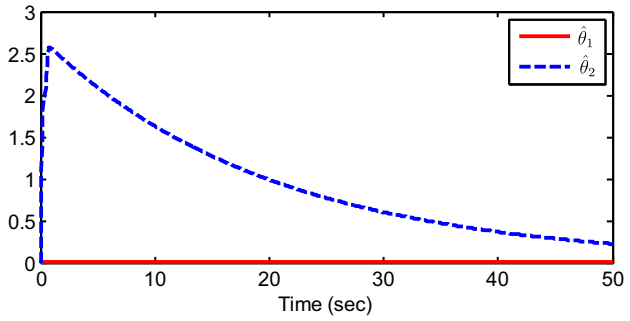

Fig. 4 The paths of the adaptive laws $\hat{\theta}_1$ and $\hat{\theta}_2$ are illustrated

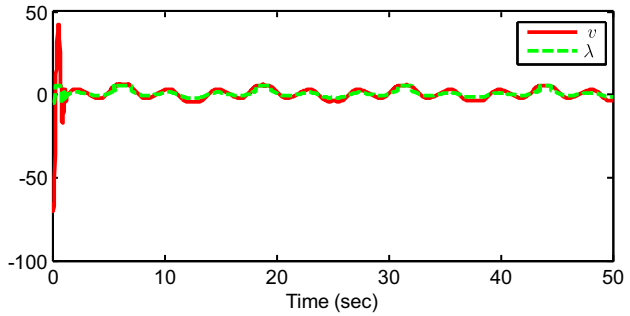

Fig. 5 The response of control input v and system input λ

Table 1 Comparative performance of the proposed method and the approach in Ref. [18]

Indexes	Case 1	Case 2
$\sum_{k=1}^{M}[y(k)-y_d(k)]^2$	6.5432	7.4568
$\sum_{k=1}^{M}[v(k)]^2$	1875.7645	1820.4219

where M indicates the total number of data points collected through sampling. These indices are assessed over a time range from 0 to 50 s, using a sampling period of 0.01 s. The results in Table 1 clearly highlight the improved effectiveness of the proposed method compared to the technique discussed in [18].

Example 2 Examine the subsequent stochastic nonstrict-feedback nonlinear system defined as

$$\begin{cases} dx_1 = (x_2 + 0.5x_1\sin(x_2))dt + (0.5x_1^2\sin(x_1))dw, \\ dx_2 = (\lambda + x_1^2\cos(x_2))dt + (x_1x_2)dw, \\ y = x_1, \end{cases} \tag{59}$$

where the state variables are denoted as x_1 and x_2, and the system input is represented by λ as defined in (2), subjected to both dead-zone and saturation effects. The reference signal is given by $y_d = 1.5\sin(0.5t)$. The input λ undergoes dead-zone and saturation nonlinearities defined as:

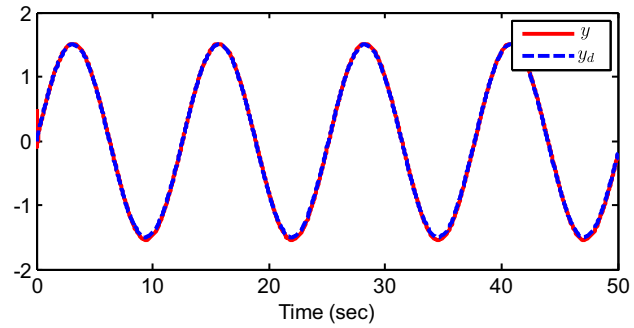

Fig. 6 Trajectories of y and y_d

$$\lambda = \begin{cases} 5, & \text{if } v > 5 \\ 0.5(v-0.5), & \text{if } 0.5 < v < 5 \\ 0, & \text{if } -0.5 < v < 0.5 \\ 0.5(v+0.5), & \text{if } -5 < v < 0.5 \\ -5, & \text{if } v < -5 \end{cases} \tag{60}$$

where $\lambda_H = 5$, $\lambda_L = 5$, $l = 0.5$, $\lambda^- = 0.5$, and $\lambda^+ = 0.5$.

The virtual controller, real controller, and adaptive laws are defined as follows:

$$\alpha_1 = -k_1\varsigma_1^{4\sigma-3} - \frac{1}{2a_1^2}\hat{\theta}_1\varsigma_1^3 S_1^T(Z_1)S_1(Z_1), \tag{61}$$

$$v = -k_2\varsigma_2^{4\sigma-3} - \frac{\hat{\theta}_2\varsigma_2^3 S_2^T(Z_2)S_2(Z_2)}{2a_2^2\rho_1}, \tag{62}$$

$$\dot{\hat{\theta}}_i = \frac{q_i}{2a_i^2}\varsigma_i^6 S_i^T(Z_i)S_i(X_i) - \gamma_i\hat{\theta}_i, \quad i = 1, 2. \tag{63}$$

The design parameters are set via trial-and-error method as follows: $q_1 = 1$, $q_2 = 2$, $a_1 = 5$, $a_2 = 2$, $\gamma_1 = 0.05$, $\gamma_2 = 0.05$, $k_1 = 50$, $k_2 = 30$, and $\sigma = \frac{99}{101}$. Utilizing a trial-and-error method, the initial conditions are established as: $[x_1(0), x_2(0)]^T = [0.5, 0.5]^T$ and $[\hat{\theta}_1(0), \hat{\theta}_2(0)]^T = [0, 0]^T$. The results of the simulation are depicted in Figs. 6, 7, 8, 9, and 10. Figure 6 illustrates the system output y alongside the desired signal y_d. The tracking error ς_1 is presented in Fig. 7, while Fig. 8 depicts the progression of the system state x_2. The responses of the adaptive laws are shown in Fig. 9, and Fig. 10 demonstrates the behavior of the control input v in conjunction with the system input λ.

In Example 1, we assess the efficacy of the proposed adaptive control method against the existing approach detailed in [18]. The pertinent results are summarized in Table 2. These metrics are computed over a time span from 0 to 50 s, utilizing a sampling interval of 0.01 s. The data presented in Table 2 clearly illustrate the enhanced performance of the proposed method relative to the one outlined in [18].

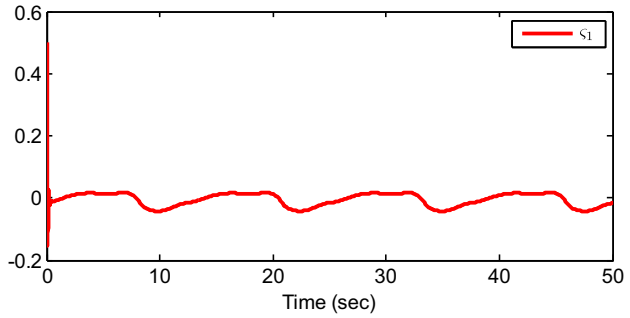

Fig. 7 The response of tracking error ς_1

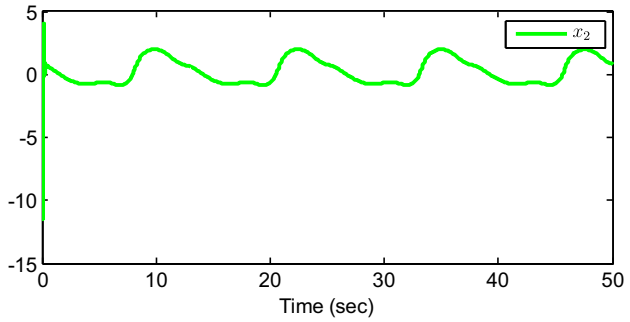

Fig. 8 The trajectories of state variable x_2

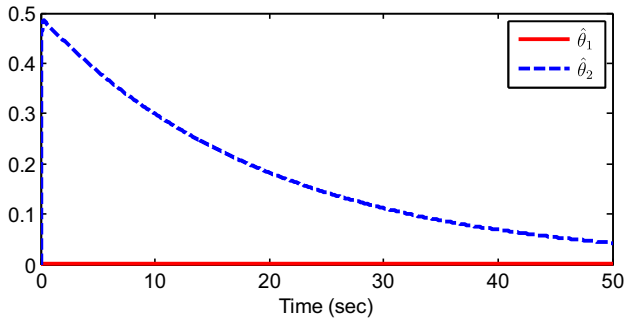

Fig. 9 The curves of adaptive laws $\hat{\theta}_1$, and $\hat{\theta}_2$

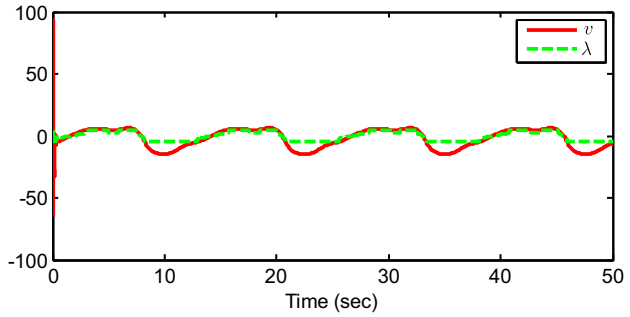

Fig. 10 The response of control input v and system input λ

Table 2 Comparative performance of the proposed method and the approach in Ref. [18]

Indexes	Case 1	Case 2
$\sum_{k=1}^{M}[y(k)-y_d(k)]^2$	5.4321	6.9876
$\sum_{k=1}^{M}[v(k)]^2$	1750.1234	1695.5678

5 Conclusion

This study introduces an adaptive finite-time tracking control strategy for stochastic systems affected by dead-zone and saturation phenomena. The approach employs neural networks (NNs) to effectively handle the unknown nonlinear functions present within the system. By applying the mean-value theorem, non-affine smooth functions are converted into an affine format, facilitating the approximation of non-smooth nonlinearities caused by input saturation and dead-zone effects. To guarantee semi-global practical finite-time stability (SGPFS) of all signals within the closed-loop system, the paper presents an adaptive finite-time controller based on the backstepping technique and finite-time stability theory. The tracking error is shown to converge to a small residual set around the origin. The proposed methodology's effectiveness is illustrated through two examples, demonstrating the controller's ability to achieve precise tracking of the reference signal with bounded error. Nonetheless, certain limitations should be acknowledged. In particular, the design parameters are determined using a trial-and-error method, which may be labor-intensive and not always result in optimal performance. Future research could aim to extend this framework to encompass higher-order stochastic systems and switched systems with full-state time-varying constraints, as well as the integration of sensor faults. Such developments would deepen the understanding of adaptive fault-tolerant control strategies for nonlinear systems and enhance their applicability in practical engineering scenarios.

Acknowledgements This work was funded by the Deanship of Graduate Studies and Scientific Research at Jouf University under grant No. (DGSSR-2024-02-02034).

Funding Open Access funding enabled and organized by Projekt DEAL.

Data Availability In this work, no underlying data were gathered or created.

Declarations

Conflict of interest The authors declare that they have no financial interests to disclose.

References

1. Hong, F.; Ge, S.S.; Lee, T.H.: Practical adaptive neural control of nonlinear systems with unknown time delays. IEEE Trans. Syst. Man Cybern. Part B Cybern. **35**(4), 849–854 (2005)
2. Chen, B.; Liu, K.; Liu, X.; Shi, P.; Lin, C.; Zhang, H.: Approximation-based adaptive neural control design for a class of nonlinear systems. IEEE Trans. Cybern. **44**(5), 610–619 (2013)
3. Sun, Y.; Chen, B.; Lin, C.; Wang, H.; Zhou, S.: Adaptive neural control for a class of stochastic nonlinear systems by backstepping approach. Inf. Sci. **369**, 748–764 (2016)
4. Park, J.-H.; Kim, S.-H.; Moon, C.-J.: Adaptive neural control for strict-feedback nonlinear systems without backstepping. IEEE Trans. Neural Netw. **20**(7), 1204–1209 (2009)
5. Zhao, X.; Wang, X.; Zhang, S.; Zong, G.: Adaptive neural backstepping control design for a class of nonsmooth nonlinear systems. IEEE Trans. Syst. Man Cybern. Syst. **49**(9), 1820–1831 (2018)
6. Min, H.; Xu, S.; Zhang, B.; Ma, Q.: Output-feedback control for stochastic nonlinear systems subject to input saturation and time-varying delay. IEEE Trans. Autom. Control **64**(1), 359–364 (2018)
7. Wang, T.; Qiu, J.; Gao, H.: Adaptive neural control of stochastic nonlinear time-delay systems with multiple constraints. IEEE Trans. Syst. Man Cybern. Syst. **47**(8), 1875–1883 (2016)
8. Wang, F.; Chen, B.; Lin, C.; Li, X.: Distributed adaptive neural control for stochastic nonlinear multiagent systems. IEEE Trans. Cybern. **47**(7), 1795–1803 (2016)
9. Zhang, T.; Xia, X.: Adaptive output feedback tracking control of stochastic nonlinear systems with dynamic uncertainties. Int. J. Robust Nonlinear Control **25**(9), 1282–1300 (2015)
10. Liu, Y.; Zhu, Q.: Adaptive neural network asymptotic tracking control for nonstrict feedback stochastic nonlinear systems. Neural Netw. **143**, 283–290 (2021)
11. Feng, Z.; Shi, P.: Sliding mode control of singular stochastic Markov jump systems. IEEE Trans. Autom. Control **62**(8), 4266–4273 (2017)
12. Xie, X.-J.; Tian, J.: State-feedback stabilization for high-order stochastic nonlinear systems with stochastic inverse dynamics. Int. J. Robust Nonlinear Control IFAC-Affil. J. **17**(14), 1343–1362 (2007)
13. Wang, T.; Zhang, Y.; Qiu, J.; Gao, H.: Adaptive fuzzy backstepping control for a class of nonlinear systems with sampled and delayed measurements. IEEE Trans. Fuzzy Syst. **23**(2), 302–312 (2014)
14. Tong Wang, J.W.; Wang, Y.; Ma, M.: Adaptive fuzzy tracking control for a class of strict-feedback nonlinear systems with time-varying input delay and full state constraints. IEEE Trans. Fuzzy Syst. **28**(12), 3432–3441 (2019)
15. Wu, L.-B.; Park, J.H.; Xie, X.-P.; Gao, C.; Zhao, N.-N.: Fuzzy adaptive event-triggered control for a class of uncertain nonaffine nonlinear systems with full state constraints. IEEE Trans. Fuzzy Syst. **29**(4), 904–916 (2020)
16. Wang, H.; Liu, S.; Yang, X.: Adaptive neural control for non-strict-feedback nonlinear systems with input delay. Inf. Sci. **514**, 605–616 (2020)
17. Ma, L.; Liu, L.: Adaptive neural network control design for uncertain nonstrict feedback nonlinear system with state constraints. IEEE Trans. Syst. Man Cybern. Syst. **51**(6), 3678–3686 (2019)
18. Han, Y.-Q.: Adaptive tracking control of a class of nonlinear systems with unknown dead-zone output: a multi-dimensional Taylor network (mtn)-based approach. Int. J. Control **94**(11), 3161–3170 (2021)
19. Yan, H.-S.; Sun, Q.-M.: Mtn output feedback tracking control for mimo discrete-time uncertain nonlinear systems. ISA Trans. **111**, 71–81 (2021)
20. Liu, L.; Cui, Y.; Liu, Y.-J.; Tong, S.: Observer-based adaptive neural output feedback constraint controller design for switched systems under average dwell time. IEEE Trans. Circuits Syst. I Regul. Pap. **68**(9), 3901–3912 (2021)
21. Tong, S.; Sui, S.; Li, Y.: Fuzzy adaptive output feedback control of mimo nonlinear systems with partial tracking errors constrained. IEEE Trans. Fuzzy Syst. **23**(4), 729–742 (2014)
22. Esfandiari, K.; Abdollahi, F.; Talebi, H.A.: Adaptive control of uncertain nonaffine nonlinear systems with input saturation using neural networks. IEEE Trans. Neural Netw. Learn. Syst. **26**(10), 2311–2322 (2014)
23. Wang, Y.; Jianbo, H.; Wang, J.; Xing, X.: Adaptive neural novel prescribed performance control for non-affine pure-feedback systems with input saturation. Nonlinear Dyn. **93**, 1241–1259 (2018)
24. Cui, G.; Jiao, T.; Wei, Y.; Song, G.; Chu, Y.: Adaptive neural control of stochastic nonlinear systems with multiple time-varying delays and input saturation. Neural Comput. Appl. **25**, 779–791 (2014)
25. Namadchian, Z.; Rouhani, M.: Observer-based adaptive neural control for switched stochastic pure-feedback systems with input saturation. Neurocomputing **375**, 80–90 (2020)
26. Zhu, Q.; Liu, Y.; Wen, G.: Adaptive neural network control for time-varying state constrained nonlinear stochastic systems with input saturation. Inf. Sci. **527**, 191–209 (2020)
27. Wang, C.; Cui, L.; Liang, M.; Li, J.; Wang, Y.: Adaptive neural network control for a class of fractional-order nonstrict-feedback nonlinear systems with full-state constraints and input saturation. IEEE Trans. Neural Netw. Learn. Syst. **33**(11), 6677–6689 (2021)
28. Ma, L.; Huo, X.; Zhao, X.; Niu, B.; Zong, G.: Adaptive neural control for switched nonlinear systems with unknown backlash-like hysteresis and output dead-zone. Neurocomputing **357**, 203–214 (2019)
29. Ma, L.; Huo, X.; Zhao, X.; Zong, G.D.: Observer-based adaptive neural tracking control for output-constrained switched mimo nonstrict-feedback nonlinear systems with unknown dead zone. Nonlinear Dyn. **99**(2), 1019–1036 (2020)
30. Ding, L.; Li, S.; Gao, H.; Liu, Y.-J.; Huang, L.; Deng, Z.: Adaptive neural network-based finite-time online optimal tracking control of the nonlinear system with dead zone. IEEE Trans. Cybern. **51**(1), 382–392 (2019)
31. Wang, H.; Karimi, H.R.; Liu, P.X.; Yang, H.: Adaptive neural control of nonlinear systems with unknown control directions and input dead-zone. IEEE Trans. Syst. Man Cybern. Syst. **48**(11), 1897–1907 (2017)
32. Tong, S.; Sui, S.; Li, Y.: Observed-based adaptive fuzzy tracking control for switched nonlinear systems with dead-zone. IEEE Trans. Cybern. **45**(12), 2816–2826 (2015)
33. Su, H.; Zhang, W.: Adaptive fuzzy control of stochastic nonlinear systems with fuzzy dead zones and unmodeled dynamics. IEEE Trans. Cybern. **50**(2), 587–599 (2018)
34. Gao, H.; Zhang, T.; Xia, X.: Adaptive neural control of stochastic nonlinear systems with unmodeled dynamics and time-varying state delays. J. Frankl. Inst. **351**(6), 3182–3199 (2014)
35. Sun, Y.; Mao, B.; Liu, H.; Zhou, S.: Output feedback adaptive control for stochastic non-strict-feedback system with dead-zone. Int. J. Control Autom. Syst. **18**(10), 2621–2629 (2020)

36. Xu, K.; Wang, H.; Zhang, Q.; Chen, M.; Qiao, J.; Niu, B.: Command-filter-based adaptive neural tracking control for strict-feedback stochastic nonlinear systems with input dead-zone. Int. J. Syst. Sci. **52**(11), 2283–2297 (2021)
37. Zhang, T.-P.; Ge, S.S.: Adaptive dynamic surface control of nonlinear systems with unknown dead zone in pure feedback form. Automatica **44**(7), 1895–1903 (2008)
38. Tong, S.; Zhang, L.; Li, Y.: Observed-based adaptive fuzzy decentralized tracking control for switched uncertain nonlinear large-scale systems with dead zones. IEEE Trans. Syst. Man Cybern. Syst. **46**(1), 37–47 (2015)
39. Wang, H.; Kang, S.; Zhao, X.; Xu, N.; Li, T.: Command filter-based adaptive neural control design for nonstrict-feedback nonlinear systems with multiple actuator constraints. IEEE Trans. Cybern. **52**(11), 12561–12570 (2021)
40. Zhang, Y.; Wang, F.: Observer-based finite-time control of stochastic non-strict-feedback nonlinear systems. Int. J. Control Autom. Syst. **19**(2), 655–665 (2021)
41. Wang, L.; Wang, H.; Liu, P.X.: Fuzzy adaptive finite-time output feedback control of stochastic nonlinear systems. ISA Trans. **125**, 110–118 (2022)
42. Min, H.; Shengyuan, X.; Zhang, Z.: Adaptive finite-time stabilization of stochastic nonlinear systems subject to full-state constraints and input saturation. IEEE Trans. Autom. Control **66**(3), 1306–1313 (2020)
43. Wang, F.; Liu, Z.; Zhang, Y.; Chen, C.L.P.: Adaptive finite-time control of stochastic nonlinear systems with actuator failures. Fuzzy Sets Syst. **374**, 170–183 (2019)
44. Shuai Sui, C.L.; Chen, P.; Tong, S.: Event-trigger-based finite-time fuzzy adaptive control for stochastic nonlinear system with unmodeled dynamics. IEEE Trans. Fuzzy Syst. **29**(7), 1914–1926 (2020)
45. Su, H.; Zhang, W.: Adaptive fuzzy control for pure-feedback stochastic nonlinear systems with unknown dead zone outputs. Int. J. Syst. Sci. **49**(14), 2981–2995 (2018)